J Mater Sci: Mater Med (2010) 21:1817–1828
DOI 10.1007/s10856-010-4053-1

In vitro dissolution of calcium phosphate-mullite composite in simulated body fluid

Ashok Priya · Shekhar Nath · Krishanu Biswas · Bikramjit Basu

Received: 4 February 2010 / Accepted: 2 March 2010 / Published online: 22 April 2010

Abstract In our recent research, we have developed novel CaP-mullite composites for bone implant applications. In order to realize such applications, the in vitro dissolution behaviour of these materials needs to be evaluated. In this perspective, the present paper reports the dissolution behavior of pure hydroxyapatite (HAp) and hydroxyapatite composites with 20–30 wt% mullite in simulated body fluid (SBF). The in vitro dissolution experiments were carried out for different time duration starting from 7 days up to 28 days. XRD and SEM results show almost no dissolution for pure HAp and HAp composite with 30 wt% mullite. However, HAp-20 wt% mullite composite exhibits considerable dissolution after 7 days. The α-TCP phase mainly contributes to the dissolution process. Based on the dynamic changes in pH, ionic conductivity, Ca and P ion concentration in SBF as well as microstructural observations of the bioceramic surfaces after various time frames of immersion in SBF, the differences in dissolution behaviour are discussed.

1 Introduction

The fundamental requirement of any biomaterial is the ability of the material to perform effectively with an appropriate host response for the desired application i.e. the material and the tissue environment of the body should coexist without having any undesirable/toxic effect [1, 2]. The body fluid constitutes water, complex compounds, dissolved oxygen and large amounts of sodium (Na^+) and chloride (Cl^-) ions, amino acids, proteins, plasma, lymph, other electrolytes, such as bicarbonate and small amounts of potassium, calcium, magnesium, phosphate, sulphate etc. [3]. Additionally, the human body environment is characterized by a salt content of about 0–9% with an average pH of 7.4 and a temperature of 37°C.

In view of the above, an important part of the research activity to develop new biocompatible materials focuses on characterizing the in vitro dissolution properties of biomaterials under scientifically controlled conditions. A synthetic analog of calcified tissues of vertebrate, hydroxyapatite (HAp) is an widely used material for bone implant applications, because HAp promotes the new bone formation, necessary for implant osseointegration [1, 4]. Additionally, the calcium phosphate (CaP) based ceramics, like HAp has beneficial osteoconductive properties to bond directly to bones, both mechanically and chemically [3]. In an in vitro study, Suzuki et al. [5] observed that the serum protein, adsorbed on the surface of tricalcium phosphate/hydroxyapatite (TCP-HAp) ceramics effectively prevented cell rupture by functioning as an intermediate layer that restricted the direct contact between cells and the material surface. Most of the calcium phosphate ceramics are resorbable and typically dissolve, when exposed to physiological environments. Some of these materials, in order of decreasing solubility include: tetracalcium phosphate ($Ca_4P_2O_9$) > amorphous calcium phosphate > α-tricalcium phosphate ($Ca_3(PO_4)_2$) > β-tricalcium phosphate ($Ca_3(PO_4)$ ≫ hydroxyapatite ($Ca_{10}(PO_4)_6(OH)_2$) [1–3]. Unlike the other calcium phosphates, hydroxyapatite does not dissolve to a great extent under physiological conditions [1]. In fact, it is thermodynamically stable at physiological pH and actively takes part in bone bonding and forms strong chemical bonds with surrounding bone. This property has been exploited for rapid bone repair after major trauma or surgery. However, HAp

A. Priya · S. Nath · K. Biswas (✉) · B. Basu
Department of Materials and Metallurgical Engineering, Indian Institute of Technology, Kanpur 208016, UP, India
e-mail: kbiswas@iitk.ac.in

has the problem of poor biodegradation, which prevents natural bone growth for extended periods [6].

The in vitro studies on HAp-based ceramics show the improvement in biocompatibility due to the formation of an apatite layer on the surface of samples triggered by addition of second phase in the HAp. Ning and Zhou [7] performed in vitro biocompatibility experiments on HAp-Ti composites containing Ti_2O, $CaTiO_3$, CaO, α-Ti and a TiP-like phase. Their results showed that the developed composites had apatite formation ability just after 2 h of immersion in SBF solution. They concluded that Ti_2O phase promoted apatite formation. Porter et al. [8] showed that addition of silicon in the hydroxyapatite led to enhanced bioactivity over pure HAp. This was attributed to the effect of silicate ions in accelerating dissolution in vitro as well as in vivo. Rameshbabu et al. [9] demonstrated that physiological stability of nanocrystalline fluorinated HAp was much higher than pure HAp. The in vitro dissolution study indicated that it was possible to fine-tune the solubility and biological lifetime by varying the amount of fluoride substitution. Gu et al. [10] investigated the in vitro dissolution and precipitation behavior of plasma sprayed yttria stabilized zirconia reinforced hydroxyapatite/Ti–6Al–4V composite coatings in simulated body fluid. The dissolution rate of composite coating was slower than that of pure HAp.

From the above-mentioned studies, it has become evident that the dissolution as well as reprecipitation of apatite crystallites promotes osseointegration. HAp bonds to the living bone through a collagen free apatite forming on the surface. The thickness, shape as well as size of the apatite depend on the characteristics of the bioactive material, such as chemical composition, surface integrity, phase assemblage present etc. The apatite can have different morphologies: porous, nodular, needlelike etc. [8, 9]. The formation of porous apatite precipitates on the sample surface leads to proliferation of osteoblast cells, because food and blood required for growth of cells can be provided by the existing bone through pores [2]. This can cause rapid tissue growth and osseointegration.

Reviewing literature, it is critically observed that no work has been reported on the in vitro dissolution study on CaP-mullite composites. This newly developed composites shows superior combination of mechanical properties like moderate hardness (∼4 GPa), and bending strength (80 MPa) with improved fracture toughness (K_{IC} ∼ 1.5 MPa $m^{0.5}$), as compared to pure HAp (K_{IC} ∼ 0.6 MPa $m^{0.5}$) and high compressive strength (∼300 MPa) [11–14]. More importantly, our recent studies reveal that these composites can exhibit good cell functionality (greater cell adhesion, proliferation and mineralization) as well as in vivo biocompatibility property [15]. Although CaP-mullite exhibits good in vivo biocompatibility, no literature report has been found to discuss the in vitro/in vivo biocompatibility of CaP-mullite composite. It is important to evaluate both in vitro and in vivo properties of any newly developed composites to enable us obtaining seamless estimation of biocompatibility. Since dissolution experiments are one of the important sets of in vitro studies, we report the in vitro dissolution study on some selected CaP-mullite composites in the present contribution. In vitro studies are also carried out keeping in mind that this will minimize the need for in vivo experiments and offer potential to study the dissolution–reprecipitation mechanism at very early time points. Previous studies have shown that simulated body fluid (SBF), which has almost the same ionic concentration as those of human blood plasma and was first used by Kokubo [16] can reproduce the in vivo responses very well in certain biomaterials [7, 8]. Therefore, investigating the biological response of any new biomaterial in SBF solution is always considered as the most effective way to predict its responses in body environment. Pure HAp was used here as baseline material in dissolution study. Mullite is a solid solution of alumina and silica with stoichiometric composition of $3Al_2O_3 \cdot 2SiO_2$. Since both Al_2O_3 and SiO_2 are biocompatible [1], it was hypothesized that mullite having Al_2O_3–SiO_2 as components also would not have any toxic effect.

2 Experimental procedure

2.1 Synthesis of materials

For the purpose of producing composites, HAp was synthesized in house by suspension precipitation method [11, 15]. In the present work, the precursor materials were calcium oxide (CaO) and phosphoric acid (H_3PO_4). Initially, CaO was dispersed in distilled water with a fixed volumetric ratio of CaO and water (18.6 g/l). The dispersed medium was kept on a hot plate and the suspension was stirred by magnetic stirrer. Following this, an appropriate concentration (0.15 M) of H_3PO_4 solution was added drop wise in the dispersed CaO medium. The temperature was kept at 80°C. The total solution was kept stirring for 3–4 h, to allow the completion of the reaction. After the reaction, the pH of the solution was adjusted to 10–12 by adding NH_4OH solution. Subsequently, the solution was kept for 1 day to precipitate the reaction product, which was collected by filtration using commercial filter paper. The precipitate was dried at 100°C for 24 h and subsequently, calcined at 800°C for 2 h. X-ray diffraction (XRD) of as- synthesized HAp, calcined at 800°C revealed the X-ray peaks corresponding to pure HAp phase [9]. Inductive coupled plasma-atomic emission spectroscopy (ICP-AES: spectroflame modula FTM08, Germany) analysis using

complexometry technique was performed to determine the Ca/P ratio of synthesized powder. Ca/P atomic ratio of 1.64 was obtained from the HAp powder calcined at 800°C [9, 10]. It is important to note that, pure stoichiometric HAp possesses a Ca/P atomic ratio of 1.67. Therefore, the as-synthesized HAp powder was quite pure and stoichiometric.

Mullite (stoichiometric composition: $3Al_2O_3{\cdot}2SiO_2$) powder was procured commercially ($D_{30} \sim 0.67$ μm, $D_{50} \sim 1.04$ μm and $D_{99} \sim 2.39$ μm, KCM Corporation, Japan) and was used as second phase reinforcement. Two different amount of mullite (20 and 30) wt% were mixed in HAp powder. The HAp-mullite composite powder mix was ball-milled for 16 h and then subsequently pressed into the forms of pellets. The sintering parameters were optimized based on the bulk density measurements and microstructure observations. The details of the densification, microstructure and process optimization could be found elsewhere [12]. Based on the sintering studies, and for the purpose of present investigation, the composites samples were sintered at 1350°C for 2 h, where as pure HAp was sintered at 1200°C for 2 h, respectively. It is to be noted that pure mullite can be sintered to full density at 1700°C, whereas fully dense HAp can be obtained at 1200°C [11]. This necessitated the sintering of HAp-mullite composition at higher temperature. The density values and sintered phases for the present set of samples are presented in Table 1. The samples are designated according to their initial composition, like HAp with x wt% mullite is designated as HApxM.

2.2 Dissolution experiments

In order to study/simulate the dissolution behavior of the CaP-mullite in physiological environment, the in vitro dissolution study was carried out by immersing three different batches of samples in Kokobu simulated body fluid (SBF) solutions for four different time periods of 7,14, 21 and 28 days. The SBF solution was prepared using the previously described method [14]. The initial pH of the solution was kept at ~7.4 with tris(hydroxymethyl)-aminomethane $[NH_2C(CH_2OH)_3]$and hydrochloric acid. The solution temperature was maintained at body temperature, i.e., 37°C using an incubator (YSI 438, Yerco Scientific India Limited). 100 ml of SBF solution was used for each sample. The ion concentration of the SBF is shown in Table 2. The solution was agitated daily to maintain uniform ion concentration. During the experiment pH of the solution was monitored every 2 days interval for about 28 days. The sample used was 4 mm $\phi \times 4$ mm cylinder. All the samples used in the study had almost same surface area and volume. One sample was taken out on 7, 14, 21 and 28 days after the start of the experiment and washed thoroughly using distilled water. The experiments were repeated for three times and characteristic behavior has been reported here.

2.3 Characterization

At the end of experiments, all the samples were rinsed gently by distilled water and then dried at 60°C for 24 h. Then the weight changes of all samples were recorded. Following this, all the experimented samples were characterized by various characterization tools. To determine the changes in phase assemblages in the sintered as well as in vitro dissolved samples, X-ray diffraction (XRD) was performed on the surface of the samples using thin film X-ray diffractometer (TF-XRD, voltage = 30 kV, current = 25 A, step size = 0.5°/min incident angle = 1°). Scanning electron microscopy (SEM, FEI SIRION, voltage = 20 kV, working distance = 8 mm) was done to reveal the changes in topographical features and to visualize the extent of dissolution in SBF. As the samples are non-conducting, gold coating for 1 min was necessary to obtain good quality images. Simultaneously, energy dispersive spectroscopic (EDS, Oxford Instruments) pattern was also recorded to identify various elements present. Fourier Transform infrared spectroscopy (FTIR, Vortex 70, Burker) of few selected samples were evaluated to get the complementary information which support XRD analysis. After the experiments, the concentrations of Ca and P ion in the SBF solution (before and after the dissolution experiments) were chemically analyzed by Atomic Absorption Spectroscopy (AAS, model Spectra AA,

Table 1 The densification, sintering conditions and phases present after sintering are mentioned against the sample designation

Samples	Maximum achievable densification (w.r.t. initial composition) %	Sintering temperatures (°C)	Phases present
Pure HAp	99.17	1200 for 2 h	HAp-ss
HAp20M	98.1	1350 for 2 h	α-TCP-ss, β-TCP-ss, HAp-ww, mullite-w, gehlenite-ww, CaO-ww, alumina-ww
HAp30M	95.6	1350 for 2 h	β-TCP-ss, α-TCP-ww HAp-ww, mullite-s, gehlenite-ww, CaO-ww, alumina-s

The phases present in the sintered body are summarized based on the XRD peak intensities

ss very strong, *s* strong, *ww* very weak, *w* weak

Table 2 Ion concentration of SBF in comparison with human blood plasma

Ion	Simulated body fluid (SBF) (mmol/l)	Human blood plasma (mmol/l)
Na^+	142.0	142.0
K^+	5.0	5.0
Mg^{2+}	1.5	1.5
Ca^{2+}	2.5	2.5
Cl^-	147.8	103.0
HCO^{3-}	4.2	27.0
HPO_4^{2-}	1.0	1.0
SO_4^{2-}	0.5	0.5

220FS). During the experiments the conductivity of the solution, pH and total dissolved solid (TDS) were dynamically measured by an electrode attached with pH meter (PC5500, Eutech Instruments).

3 Results

3.1 Phase assemblage

Figures 1 and 2, illustrate the phase assemblages present in pure HAp and HAp20M composites after sintering as well as various dissolution periods (7, 14, 21 and 28 days). Figure 1 shows the comparison of phases when pure hydroxyapatite (HAp) samples were soaked in SBF from 0 to 28 days with 7 days interval. The XRD pattern collected from sintered sample (bottom spectrum of Fig. 1) reveals that all the peaks can be identified of pure HAp phase (hexagonal, $a = 0.943$ nm, $c = 0.688$ nm). XRD patterns collected from each time period sample clearly reflect the fact that there is no visible change in phase assembly during the time scale of the dissolution test. The peak position and relative intensity remain unchanged during the dissolution test.

In contrast, HAp20M sintered composite (bottom spectra of Fig. 2 contain mainly β-tricalcium phosphate (β-TCP, rhombohedral, $a = 1.0435$ nm, $c = 3.7403$ nm) and mullite (orthorhombic, $a = 0.755$ nm, $b = 0.769$ nm and $c = 0.288$ nm) as major phases along with α-tricalcium phosphate (α-TCP, monoclinic, $a = 1.289$ nm, $b = 2.728$ nm, $c = 1.522$ nm and $\beta = 126.2°$) and HAp. It is clear that TCP phases are formed because of dissociation of HAp during sintering [14]. XRD patterns of the composite also show the presence of other dissociation products of HAp, CaO and reaction product; gehlenite ($2CaO{\cdot}Al_2O_3{\cdot}SiO_2$, tetragonal, $a = 0.759$ nm and $c = 0.490$ nm) in the as sintered sample. The details of phase assemblages and sintering condition optimization can be found elsewhere [7]. Table 1 describes presence of different phases in the pure HAp as well as composite samples. XRD pattern of sintered HAp30M composite (not shown here) indicates number and intensity of α-TCP peaks to be very small as compared to HAp20M sample. The presence of β-TCP peaks is evident in HAp30M composites.

Figure 2 depicts the dissolution behaviour in Kokubo solution as a function of time for HAp20M composites. One can clearly observe that the intensity of α-TCP peaks (marked on Fig. 2) in HAp20M sample reduces from 7 to 28 days of dissolution. Comparing from Fig. 2, it is also

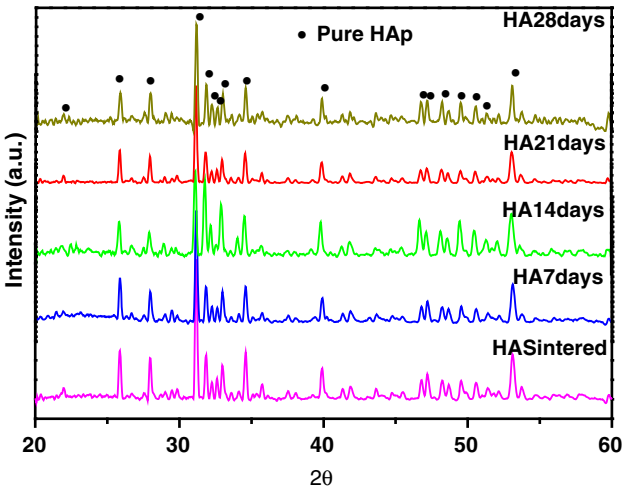

Fig. 1 XRD diagrams acquired from the surface of pure hydroxyapatite sample after the dissolution test for various time duration. XRD from the as sintered sample is also included for comparison

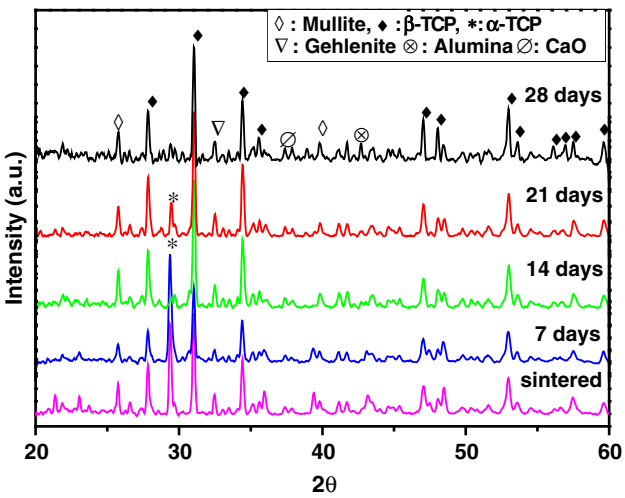

Fig. 2 XRD diagrams acquired from the surface of HAp20M sample after the dissolution test for various time duration. XRD from the as sintered sample is also included for comparison

quite evident that the α-TCP phase is dissolving with time in both cases. The other sintered phases like mullite, alumina, gehlenite do not show any dissolution as there is almost no change in their corresponding peak height relative to the strongest peak. The detailed intensity calculations indicate that CaO peak intensity decreases as function of immersion time. Similar behaviour has been observed for HAp30M sample during in vitro dissolution test.

3.2 Microstructural observation

We will now discuss the scanning electron microscopic (SEM) observations of the three samples as a function of immersion time. Figure 3 describes the as-sintered microstructures (prior to dissolution experiment) of pure HAp (a), HAp20M (b) and HAp30M (c, d) samples. Figure 3a shows nearly pore free equiaxed grainy microstructure of pure HAp sintered at 1200°C for 2 h. The microstructure is characterized by bimodal grain distribution with coarser grains of 5–6 μm and finer grains of 1–2 μm. Figure 3b reveals the as-sintered microstructure of HAp20M sample, sintered at 1350°C for 2 h. This microstructure is quite different than that of pure HAp. Here, the calcium phosphate (HAp/TCP) phases form the matrix and mullite along with other dissociation and reaction products spread homogeneously throughout the microstructure. The different phases are marked on the microstructure. Mullite is characterized by needle shaped morphology (marked by arrow on the figure). The dissociation products as well as the reaction products are found to form along the grain boundaries of calcium phosphate phases. Inset in Fig. 3b clearly shows the presence of such phases. Similar microstructural observation could be made for HAp30M sample (Fig. 3c) as well. Here, as the mullite content is higher and therefore, apparent volume fraction of grain boundary phase is more than that of HAp20M. Figure 3d shows the high magnification image of HAp30M sample. This image shows the presence of the grain boundary phases in calcium phosphate matrix.

After 7 days of dissolution experiment, the microstructural observations are shown in Fig. 4. For pure HAp, there is some visible change in the microstructure after 7 days (Fig. 4a). Low magnification microstructure reveals equiaxed grain morphology with precipitation of apatite crystallites on the sample surface. The apatite precipitates are composed of agglomerated nodular shaped crystals. Detailed observation shows small dissolved regions from very few-selected zone of the microstructure (inset of Fig. 4a). However, the number of such dissolved regions is very few and is not distributed homogenously in the sample. Similarly, for HAp20M and HAp30M sample, the microstructures (Fig. 4b, c, respectively) reveal that the samples are unaffected after 7 days of dissolution. No visible effect of dissolution can be observed for HAp20M sample. However, both HAp20M as well as HAp30M sample show precipitation of apatite deposits on few areas of microstructure. The precipitation of apatite is more prevalent in HAp30M sample. Figure 4d reveals higher magnification micrograph of the region marked in Fig. 4c. The needle-like crystallite, agglomerated is observed on the surface of the sample. The EDS pattern (Fig. 4e) taken from such regions reveals presence of Ca, P, Si, Al and O. The composition analysis suggests 59.3 wt%Ca, 6.9 wt%Si, 26.7 wt%P, 7.1 wt%Al.

After 14 days, microstructure of pure HAp sample shows clusters of apatite precipitate on the surface (Fig. 5a) with inset showing one such apatite precipitate. In some regions, the surfaces of the HAp grains appear mottled (marked on the figure), suggesting the occurrence of dissolution. Many apatite deposits are associated with HAp grains, which exhibit mottled contrast. There is considerable change in HAp20M microstructure. Figure 5b shows low magnification microstructure of HAp20M with large number of dissolved regions distributed throughout the microstructure. Figure 5c presents high magnification image of one such dissolved region, which reveals that the matrix is dissolved though the grain boundary phases remain like skeleton. The 'circle' marked region of Fig. 5c shows the area about to begin dissolution. Figure 5e plots the EDS pattern collected from Fig. 5c. The presence of elements like Ca, P, Al, Si and O resemble as sintered composite microstructure. Au peak is due to gold coating used for observation of the sample under SEM. In contrast, no dissolution could be observed in case of HAp30M sample (Fig. 5d).

After 21 days, there is minimal dissolution form pure HAp (Fig. 6a). The white arrow on the figure indicates higher magnification image of one such dissolved region. The nodular apatite crystals are also observed (marked on the figure). SEM images obtained from the HAp20M surface show (Fig. 6b) more dissolution as the number and size of the dissolved areas increase. Higher magnification microstructure (Fig. 6c) of a dissolved region with EDS analysis from the dissolved skeleton. Like in the previous case, one can clearly observe the dissolution of the matrix phase leaving behind the skeleton of grain boundary phases. One can also observe mullite needles in the dissolved region. The EDS analysis reveals the dominant presence of Al, Si, Ca and O. The P peak is negligible compared to other elements. The HAp30M sample does not exhibit any dissolution (Fig. 6d). However, reprecipitation of apatite has been found to occur on the sample surface. The EDS pattern in right inset of Fig. 6d shows the spectra collected from one such apatite precipitate, revealing the predominant presence of Ca, P, Al and O.

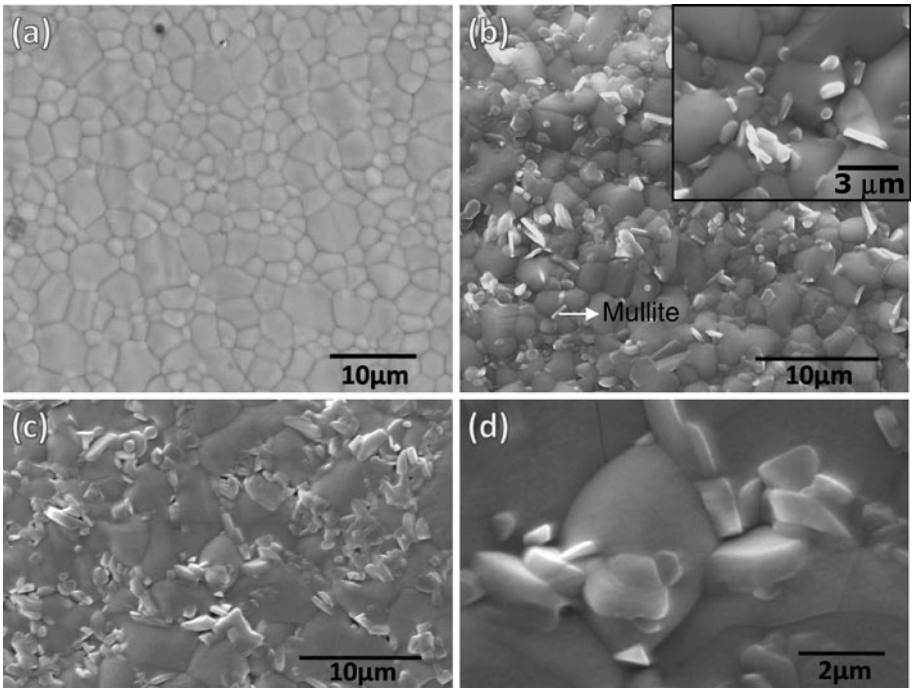

Fig. 3 SEM images shows the topographic features of **a** pure HAp, **b** HAp-20M, **c** HAp-30M, **d** closer look of HAp30M samples sintered at optimum condition

After 28 days of experiment, pure HAp shows (Fig. 7a) negligible dissolution in some regions on the sample surface. Some of dissolved regions are also marked on the micrograph. The formation of apatite is found to be uniform on the HAp grains. Some of these apatite precipitates are very (inset of Fig. 7a) large. In many cases, the dissolution and reprecipitation of apatite appears to be more extensive here and nodular apatite deposits have formed in the vicinity of the dissolved areas on the surface of the HAp grains. However, HAp20M (Fig. 7b) does not dissolve further after 28 days as compared to 21 days sample. There is some deposition is observed on the dissolved area (marked on Fig. 7b). Interestingly, in very few areas, HAp30M samples also show single grain dissolution (Fig. 7c) as well as reprecipitation of apatite in several regions on the sample surface. The higher magnification image (inset of Fig. 7c) of the dissolved area clearly indicates the nature of single grain dissolution. This is quite different from HAp20M sample.

3.3 Chemical analysis

The dissolution behaviour of the samples in Kokubo SBF solution can be determined by measuring the Ca^{2+} and P^{3+} ion concentration in the SBF solution during the experiment using atomic absorption spectroscopy. Figure 8a shows the ratio of Ca^{2+} ion concentration in the SBF during the 28 days period with intervals of 7 days. It is clear that during initial period of 7 days, the Ca^{2+} ion concentration decreases for all samples. After that, Ca^{2+} concentration increases sharply in the solution containing HAp30M sample. For in vitro solution with pure HAp and HAp20M samples, Ca^{2+} ion concentration decreases further till 14 days. This is followed by the increase in Ca^{2+} ion concentration of these two samples, following the similar slope that of HAp30M sample. After 21 days the Ca^{2+} ion concentration again decreases for HAp30M sample. However, the Ca^{2+} ionic concentration stabilizes for pure HAp and HAp20M samples containing solution. Throughout the experimented time regime, the behavior of Ca^{2+} ion concentration plots for pure HAp and HAp20M are quite similar.

In contrast, dissimilar results are observed for P^{3+} ion concentration plot (Fig. 8b). Herein, the P^{3+} ion concentration increases during initial 7 days for pure HAp. However, the P^{3+} ion concentration decreases for mullite containing samples during 21 days of dissolution. The P^{3+} ion concentration decreases at a faster rate for HAp20M sample than HAp30M sample. After 21 days, while the P^{3+} ion concentration of HAp30M sample containing solution continue to decrease with similar rate, the P^{3+} ion concentration of HAp20M containing solution abruptly increase at 28th day of experiments. For pure HAp, the P^{3+} ion concentration decreases at 14th day and again increases minutely at 21st and 28th day of experiment.

3.4 pH and conductivity of the solution

To obtain further insight into the dissolution, pH and ionic conductivity of the solution were recorded. The data were collected for up to 28 days with periodic interval of

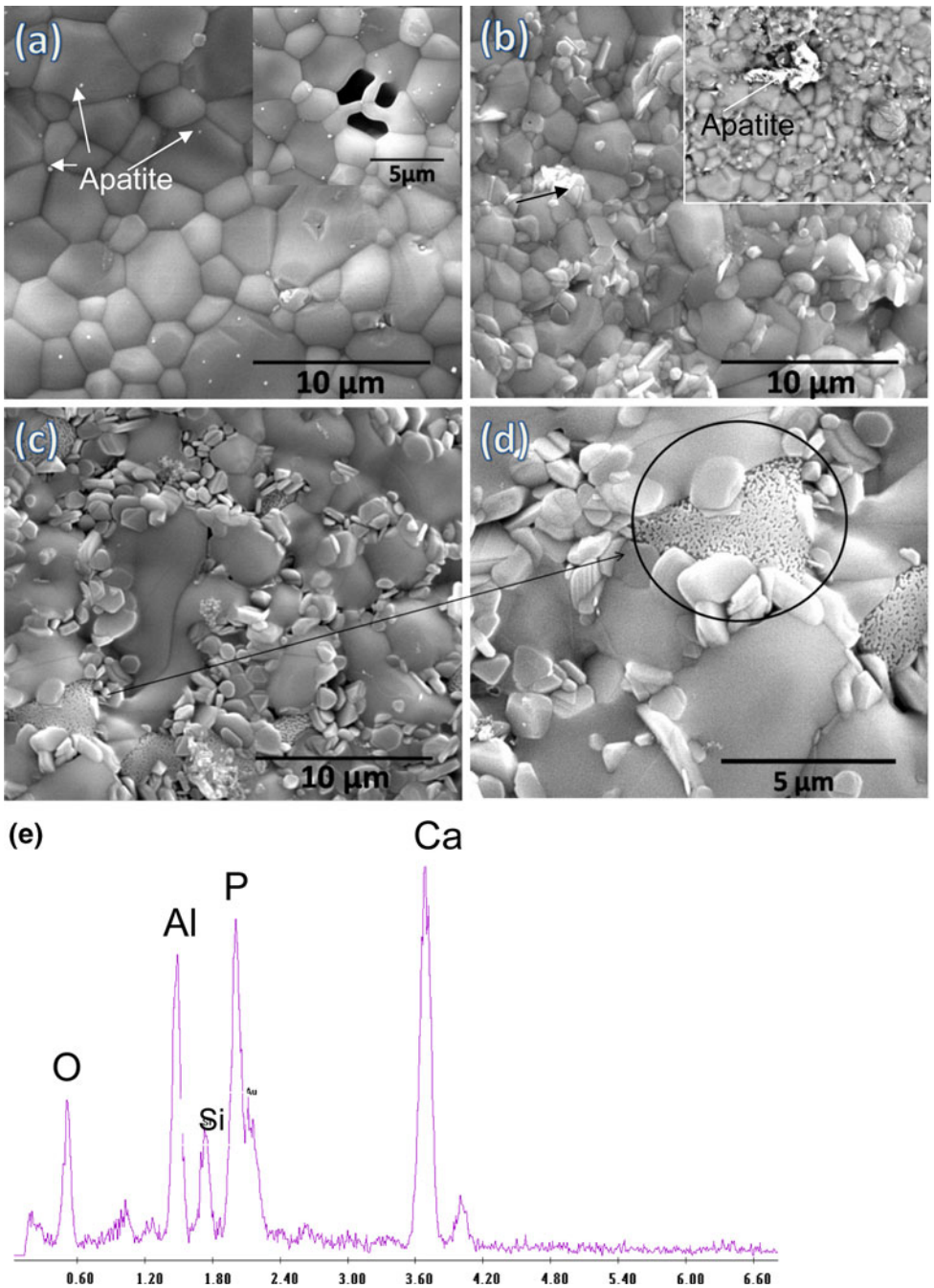

Fig. 4 SEM images show the topographical features of **a** pure HAp, **b** HAp-20M, **c**, **d** HAp30M samples, after 7 days of dissolution period, **d** shows a magnified zone of (**c**) marked by *arrow*, **e** EDS profile taken from the magnified zone

2 days. The starting pH value of the solution was ~7.4. Up to 12 days, the pH values for all the samples fluctuate in between 7.35 and 7.55. After 12 days, sharp decrease in pH value of the solution irrespective of samples is noticed. The pH values then stabilize at 7.2 and the values fluctuate in between 7.15 and 7.3 till 28 days. Similar trends could be observed for conductivity measurement. The conductivity of all solutions decreases steeply after 12 days and stabilizes during the timeframe of 14–28 days.

4 Discussion

We shall discuss the results obtained during in vitro dissolution study of pure HAp as well as composites in the light of the following aspects:

(a) Formation of apatite phase in different materials.
(b) Change in morphology of apatite crystals/layer with time duration of dissolution.
(c) Dissolution behaviour.

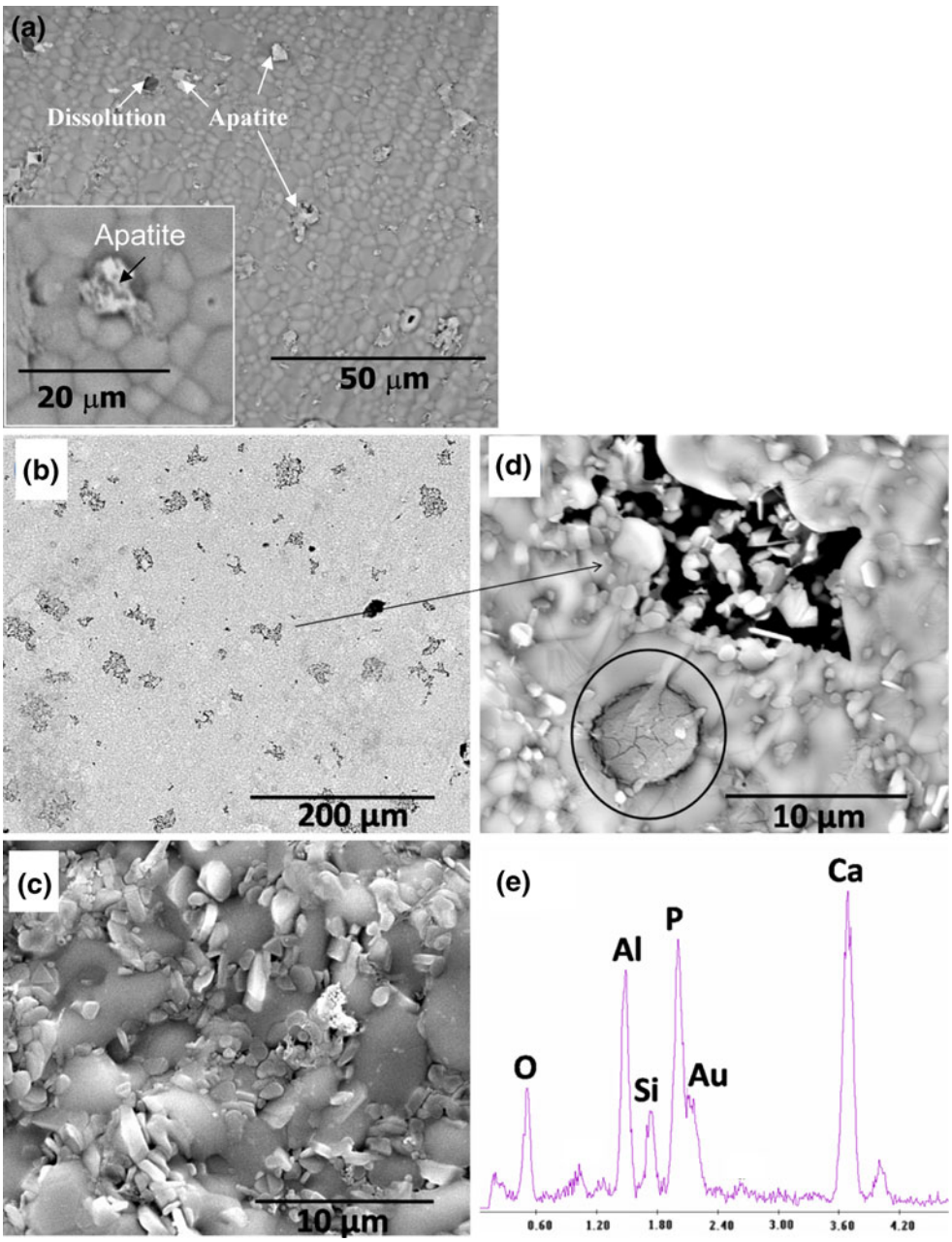

Fig. 5 SEM images show the topographical features of **a** pure HAp and **b** HAp-20M, **c** HAp30M samples, after 14 days of dissolution period, **d** is a magnified image of a selected zone from (**b**), **e** shows the EDS spectra collected from full frame image of (**c**)

It is well known in the literature that SBF can be kept for at least 2 months at physiological temperature without any precipitation [6–9]. Therefore, SBF is quite stable at 37°C. So, the formation of apatite on the surfaces of HAp and composites during the experiment must be linked towards interactions between the investigated materials and SBF. From SEM observations and XRD plots, it is quite clear that pure HAp does not undergo extensive dissolution even after 28 days of experiments. This is quite likely as HAp is stable at pH $>$ 7.2. The microstructural observation, indicating dissolution at beginning as mentioned in Fig. 4a is only limited to small regions of the sample. However, in some regions (in Figs. 5a, 6a), the surfaces of HAp grains appear to be mottled, which is a signature that dissolution has occurred. In many cases, the mottled contrast is present throughout the grain; otherwise part of the grain shows mottled contrast. Precipitation of nodular and flaky apatite has been found on the HAp grains, which have agglomerated in mottled regions of the sample surface. With the increase in immersion time, the quantity and size of these apatite particles increase gradually. After 28 days, both dissolution and reprecipitation of apatite mineral are more prevalently observed. XRD results (Fig. 1) show almost no change in the XRD spectra of HAp samples recorded for

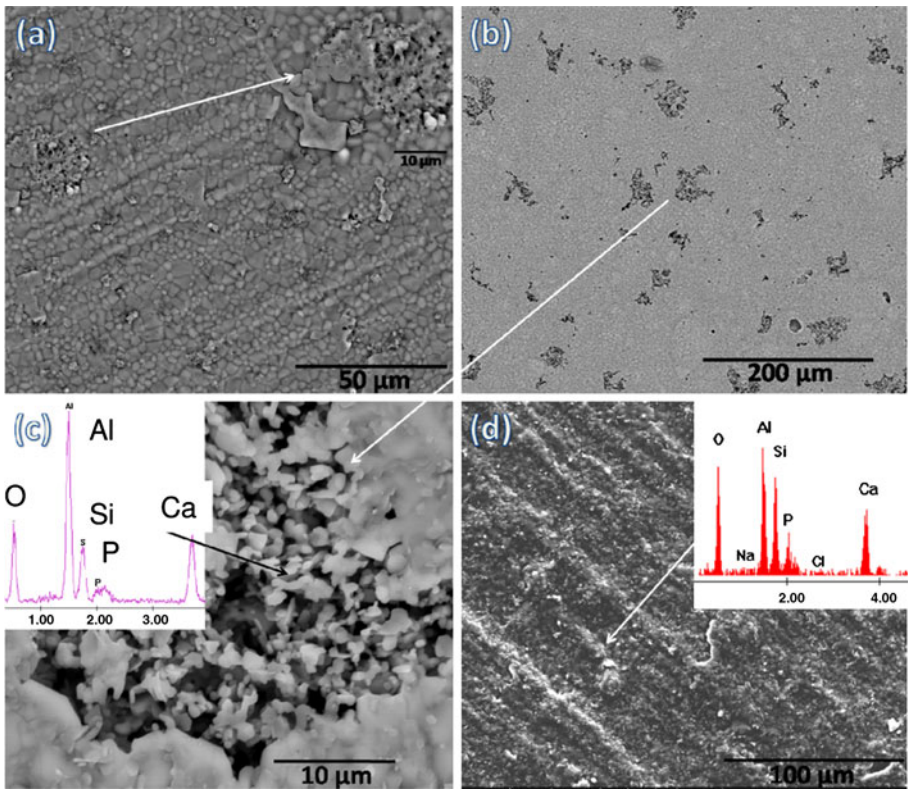

Fig. 6 SEM images show the topographical features of **a** pure HAp, **b**, **c** HAp-20M, **d** HAp-30M samples, after 21 days of dissolution period. In (**a**) the *inset* shows a specific observation. In (**c**, **d**) the *insets* show the EDS counts from the *arrow* marked zone

various time intervals during the experiment. The amount of the apatite precipitates has not been sufficient enough to be detected by XRD. It is to be that the formation of apatite on sample surface is prevalent in both the composites. HAp20M reveals formation of flaky apatite on the sample surface whereas HAp30M shows formation of porous nodular apatite agglomerate beginning just after 7 days of immersion in SBF. The area fraction of the apatite agglomerate in both cases increases with immersion time.

It has been shown in the literature that the formation of the collagen-free apatite layer is an essential requirement for osseointegration of the implant [5–8]. The bioactivity of calcium phosphate and other materials has been related to their propensity to nucleate apatite crystals. The presence of bone-like apatite agglomerate on the surface of any implant is always considered as a positive biological response from host tissue. Therefore, pure HAp and composites, in the present case, showing extensive precipitation of apatite is a clear indication of bioactivity. In fact the formation of porous apatite agglomerate in case of HAp30M is beneficial for the proliferation of biological cells from the existing bone near the implant. This is because of the fact that food and blood circulation required can easily be provided through these porous apatite crystals.

Let us now discuss the dissolution of phase during in vitro study. HAp20M and HAp30M samples mainly contain β-TCP and mullite as major phases. In HAp20M sample, α-TCP is also present as major phase, whereas, α-TCP is a minor phase in HAp30M sample. The diffractograms also show traces of CaO, Al_2O_3 and gehlenite. For HAp20M sample, the intensities of α-TCP and CaO peaks decrease with an increase in immersion period. The formation of TCP, CaO and Al_2O_3 have formed during dissociation of HAp at high temperature during sintering [9, 12]. The higher dissolution of HAp20M sample could be attributed to the presence of metastable phase, α-TCP. The dissolution of HAp20M sample starts from 7 days and continue till 21 days. With the increase in immersion period in SBF, α-TCP peak intensity decreases and after 28 days, α-TCP peaks almost disappear from sample surface. CaO peak intensity (relative to the most intense peak of β-TCP peak) also decreases substantially in HAp20M sample after 28 days of immersion in SBF. The dissolution of α-TCP and CaO phases can be explained by reaction of these phases in SBF solution as per the following reaction pathways [8, 9]:

$$4Ca_3(PO_4)_3 + 4H_2O \Leftrightarrow Ca_{10}(PO_4)_6(OH)_2 + 2Ca^{2+} + 6HPO_4^{2-} \quad (1)$$

$$HPO_4^{2-} \Leftrightarrow H^+ + PO_4^{3-} \quad (2)$$

$$CaO + H_2O \Leftrightarrow Ca^{2+} + 2OH^- \quad (3)$$

According to Eq. (3), formation of OH^- should lead to increase in pH value of the SBF. On the other hand, H^+

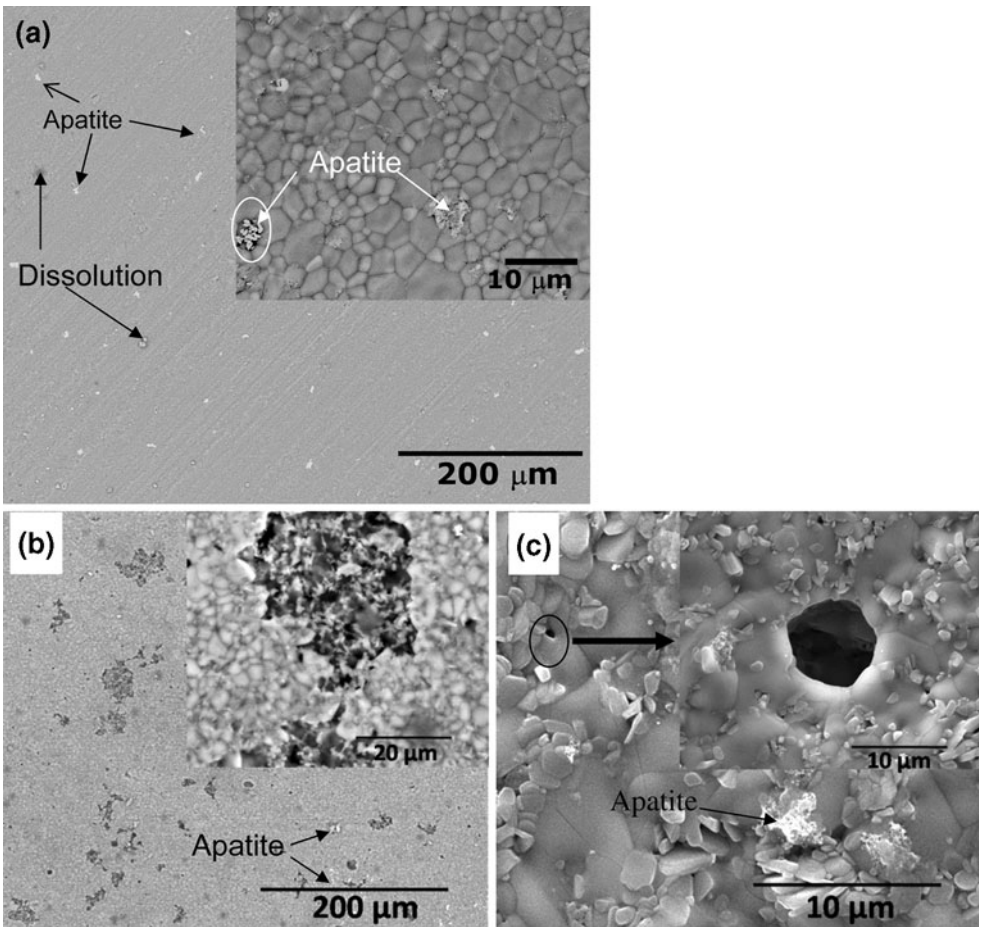

Fig. 7 SEM images show the topographical features of **a** pure HAp, **b** HAp-20M, **c** HAp-30M samples, after 28 days of dissolution period. In (**a**–**c**) the *inset* shows a specific observation

ions are generated by reaction (2). It is to be noted that the dynamic nature of dissolution process will essentially results in changes of H^+ and OH^- ion concentration. We observe increase of pH of SBF solution in the first 2 weeks (from 7.4 to 7.5 for HAp30M and 7.4 to 7.45 for HAp20M) for the composite samples due to increase in OH^- ion concentration. In case of pure HAp, pH deceases initially (up to 7 day) because of absence of any CaO. As CaO is a minor phase in the composite, the change in pH of the SBF is small. The presence of larger volume fraction of α-TCP in comparison to CaO leads to more amount of H^+ ions and thereby, the solution becomes more acidic with the immersion time. pH of SBF solution for composites drops after 14 days due to precipitation of apatite requiring OH^- for the same. This also leads to reduction of OH^- ions in the SBF solution. This reprecipitation of apatite is found to take place for both pure HAp and the composites. TDS measurements reveal similar trends for pure HAp as well as composites.

It has been observed that the insoluble parts of the microstructure remains as dissolution process leaves a skeleton of grain boundary phases in HAp20M composites. α-TCP is present in HAp30M as minor phase. The amount of CaO is also found to be very small as compared to other phases. Therefore, HAp30M samples do not undergo much dissolution. It is already known that both β-TCP and α-TCP are soluble in SBF [1, 5–8]; however, β-TCP is quite stable phase at ambient condition. β-TCP does not show any dissolution (for both HAp20M and HAp30M samples) during the experimented time frame. It is possible that the faster soluble α-TCP phase increases the P concentration in the solution and hence, lowers the dissolution kinetics of β-TCP. Although the dissolution of the metastable phases begins from the first week of immersion, extensive dissolution takes place from second week, releasing calcium and phosphorous ions into the solution. This, in turn increases supersaturation in the solution and thus precipitation of the apatite into the surface of HAp20M and HAp30M samples occurs by consuming the calcium and phosphorous ions from the solution. It is to be noted that the dissolution and reprecipitation is a dynamic process. In the beginning, the dissolution rate is lower than the reprecipitation and calcium and phosphorous ion concentration decrease in the solution. After 2 weeks, rate of dissolution takes over the reprecipitation, and the calcium and phosphorous ion concentration in the SBF solution increase.

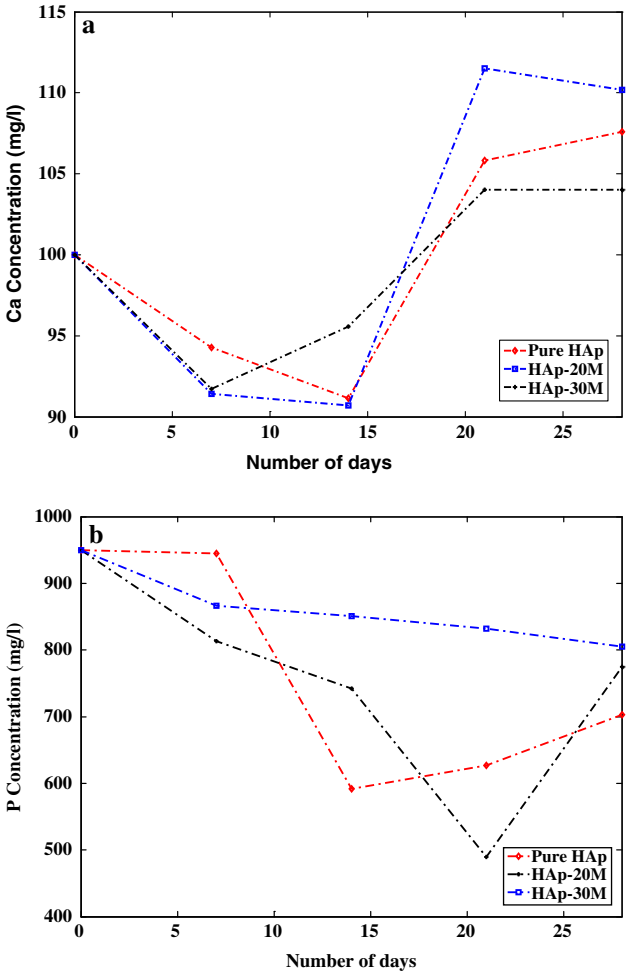

Fig. 8 **a** Ca^{2+} ion concentration in the solution for various samples after stipulated time period, **b** P^{3+} ion concentration in the solution for various samples after stipulated time period

Comparing the weight measurements of the samples before and after the in vitro tests, a considerable amount of weight loss was observed for HAp20M sample over the experimented time frame. This result supports the microstructure observation and XRD analysis. Also, for pure HAp and HAp30M the weight change is negligible till 21 days. After 21 days, the sharp weight loss of HAp30M sample could be attributed to the late stage dissolution, which was also revealed from Figs. 4, 5, 6, 7. In case of pure HAp, sample gains small weight later because of precipitation of apatite layer during immersion being larger than dissolution.

One of the notable finding of the present investigation is the extensive dissolution of HAp20M composite as compared to pure HAp and HAp30M. This result has a lot of implication as far as potential application of the novel composite is concerned. Although pure HAp has osteoconductive properties similar to bone allowing it to bond well with bone, it has the problem of poor biodegradability [1]. Therefore, it prevents the natural bone regrowth for extended period. TCP, on the other hand, is bioactive as well as biodegradable material, which will allow it to induce bone regrowth without changing much the osteoconductive property. This is very much evident from our study. The dissolution of α-TCP during immersion will further improve bone regrowth because the new bone cells (osteocytes, osteoblast) can easily attach themselves in the dissolved regions. The rough surfaces created due to dissolution, can provide sites for bone regrowth, which will cause mechanical interlocking and bony union with the implant resulting in high interfacial strength between the existing bone and the implant. For examples, Fig. 5c clearly illustrate as how larger size (∼10–30 μm) porous regions were developed during dissolution process. The formation of such porous regions, coupled with nodular apatite regions will act as precursor to osseointegration process. Therefore, HAp20M and HAp30M have greater biological efficacy in terms of osteoblast adhesion, proliferation and formation of bones tissue in-growth and thus, potential to be used as bone repair and replacement application as compared to pure HAp.

5 Conclusions

The major conclusions of the present investigation are as follows:

(a) One of the important observations is that the investigated calcium phosphate-mullite composites are capable of producing porous apatite layer in vitro. The combination of dissolution and reprecipitation are found to be the mechanism of apatite formation. The apatite layer formation is expected to encourage the osseointegration of the investigated bioceramic composites.

(b) After longer duration of dissolution, HAp20M composite reveals the formation of macroporous regions in the composites because of considerable dissolution due to the presence of α-TCP and CaO phases.

(c) Formation of such macroporous regions and rough surface created during dissolution will allow proliferation of biological cells by providing mechanical interlocking and bony union of the implant.

(d) HAp20M and HAp30M composites show greater biological efficiency as far as proliferation of biological cell and bone in growth are concerned.

Acknowledgment The authors would like to acknowledge the funding agency, Department of Biotechnology, Govt. of India for financial assistance under the project DBT/MET/20090134.

References

1. Thamaraiselvi TV, Rajeswari S. Biological evaluation of bioceramic materials—a review. Trends Biomat Artif Org. 2004; 18(1):9–17.

2. Nath S, Basu B. Designing biomaterials for hard tissue replacement. J Kor Cer Soc. 2008;45(1):1–29.
3. Kong Y-M, Bae C-J, Lee S-H, Kim H-W, Kim H-E. Improvement in biocompatibilty of zirconia-alumina nanocomposite by addition of HA. Biomaterials. 2005;26:509–17.
4. Hench LL. Bioceramics. J Am Ceram Soc. 1998;81:1705–28.
5. Suzuki T, Ohashi R, Yokogawa Y, Nishizawa K, Nagata F, Kawamoto Y, et al. Initial anchoring and proliferation of fibroblast L-929 cells on unstable surface of calcium phosphate ceramics. J Biosci Bioeng. 1999;87(3):320–7.
6. Adolfson E, Peter A-H, Hermannson L. Phase analysis and thermal stability of hot isostatically pressed zirconia-hydroxyapatite composites. J Am Ceram Soc. 2000;83(11):2798–802.
7. Ning CQ, Zhou Y. In vitro bioactivity of a biocomposite fabricated from HA and Ti powder metallurgy method. Biomaterials. 2002;23:2909–15.
8. Porter AE, Botello CM, Lopes MA, Santos JD, Best SM, Bonfield W. Ultrastructural comparison of dissolution and apatite precipitation on V and silicon-substituted hydroxyapatite in vitro and in vivo. J Biomed Mater Res A. 2004;69A:670–9.
9. Rameshbabu N, Sampath Kumar TS, Prasad Rao K. Synthesis of nanocrystalline fluorinated hydroxyapatite by microwave processing and its in vitro dissolution study. Bull Mater Res. 2006; 29(6):611–5.
10. Gu YW, Khor KA, Pan D, Cheang P. Activity of plasma sprayed yttria stabilized zirconia reinforced Hydroxyapatite/Ti-6Al-4V composite coatings in simulated body fluid. Biomaterials. 2005;25: 3177–85.
11. Nath S, Biswas K, Basu B, Wang K, Bordia RK. Sintering and phase stability in hydroxyapatite-mullite system. J Am Cer Soc 2009. doi:10.1111/j.1551-2916.2010.03662.x.
12. Nath S. Development of novel calcium phosphate-mullite composite for orthopedic applications. Ph.D Thesis, 2008, Indian Institute of Technology, Kanpur, India.
13. Nath S, Dey A, Mukhopadhyay AK, Basu B. Nanoindentation response of noval hydroxyapatite-mullite composites. Mat Sci Eng A. 2009;513–514:197–201.
14. Nath S, Biswas K, Basu B. TEM study of dissociation and thermochemical compatibility in HAp-mullite system. Scripta Mater. 2008;58:1054–7.
15. Nath S, Basu B, Mohanty M, Mohanan PV. In vivo response of novel hydroxyapatite -mullite composites: results up to 12 weeks of implantation. J Biomed Mater Res B. 2009;90B:547–57.
16. Kokubo T, Kushitani H, Sakka S, Kitsugi T, Yamamuro T. Solutions able to reproduce in vivo surface-structure changes in bioactive glass-ceramic A-W[3]. J Biomed Mat Res. 1989;24:721–34.